

D²LV: A Data-Driven and Local-Verification Approach for Image Copy Detection

Wenhao Wang, Yifan Sun, Weipu Zhang, Yi Yang
Baidu Research

wangwenhao0716@gmail.com, sunyifan01@baidu.com, zhangweipu01@baidu.com, yee.i.yang@gmail.com

Abstract

Image copy detection is of great importance in real-life social media. In this paper, a data-driven and local-verification (D²LV) approach is proposed to compete for Image Similarity Challenge: Matching Track at NeurIPS'21. In D²LV, unsupervised pre-training substitutes the commonly-used supervised one. When training, we design a set of basic and six advanced transformations, and a simple but effective baseline learns robust representation. During testing, a global-local and local-global matching strategy is proposed. The strategy performs local-verification between reference and query images. Experiments demonstrate that the proposed method is effective. The proposed approach ranks first out of 1,103 participants on the Facebook AI Image Similarity Challenge: Matching Track. The code and trained models are available [here](#).

1. Introduction

The goal of image copy detection is to determine whether a query image is a modified copy of any images in a reference dataset. It has extensive numbers of applications, such as checking integrity-related problems in social media. Although this topic has been researched for decades, and it has been deemed as a solved problem, most state-of-the-art solutions cannot deliver satisfactory results under real-life scenarios [8]. There are two main reasons. First, real-life cases in social media involve billions to trillions of images, which introduces many “distractor” images to degrade the performance. Second, the transformations used to edit images are countless. It is very challenging for an algorithm to be robust to unseen scenarios.

In this paper, a data-driven and local-verification (D²LV) approach is proposed to compete for Image Similarity Challenge: Matching Track at NeurIPS'21 (ISC2021) [8]. This competition builds a benchmark that features a variety of image transformations to mimic real-life cases in social media. To mimic a needle-in-haystack setting, both the query and reference set contain a majority of “distractor” images that do not match. The evaluation metric adopted is micro

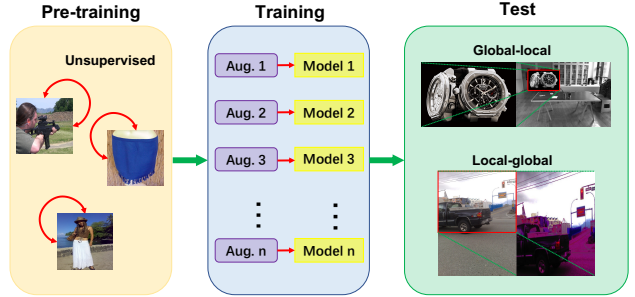


Figure 1. The data-driven and local-verification approach. Unsupervised pre-training is used to substitute supervised one. During training, we get different trained models by designing different sets of augmentations. Global-local and local-global matching strategy is proposed for testing.

Average Precision, which penalizes any detected pair for a distractor query.

The approach consists of three parts, *i.e.* pre-training, training, and test. In pre-training, unsupervised pre-training on ImageNet [6] instead of the commonly-used supervised pre-training is performed. Specifically, we empirically find that BYOL [13] pre-training (its Momentum² Teacher version [19]) and Barlow-Twins [37] pre-training are superior to some other unsupervised pre-training methods, and a further ensemble of these two is even better. In training, a strong but simple deep metric learning baseline is designed by combining both the classification loss and the pairwise loss (triplet, in particular). Moreover, to make the sample pairs more informative, a battery of image augmentations is employed to generate training images. Empirically, we find that different augmentations may disturb each other to degrade the performance. Therefore, we use different sets of augmentations to train models separately and then ensemble them. The diversity of augmentations promotes learning robust representation. During testing, a robust global-local and local-global matching strategy is proposed. We observe two hard cases: a) some query images are generated by overlaying a reference image on top of a distractor im-

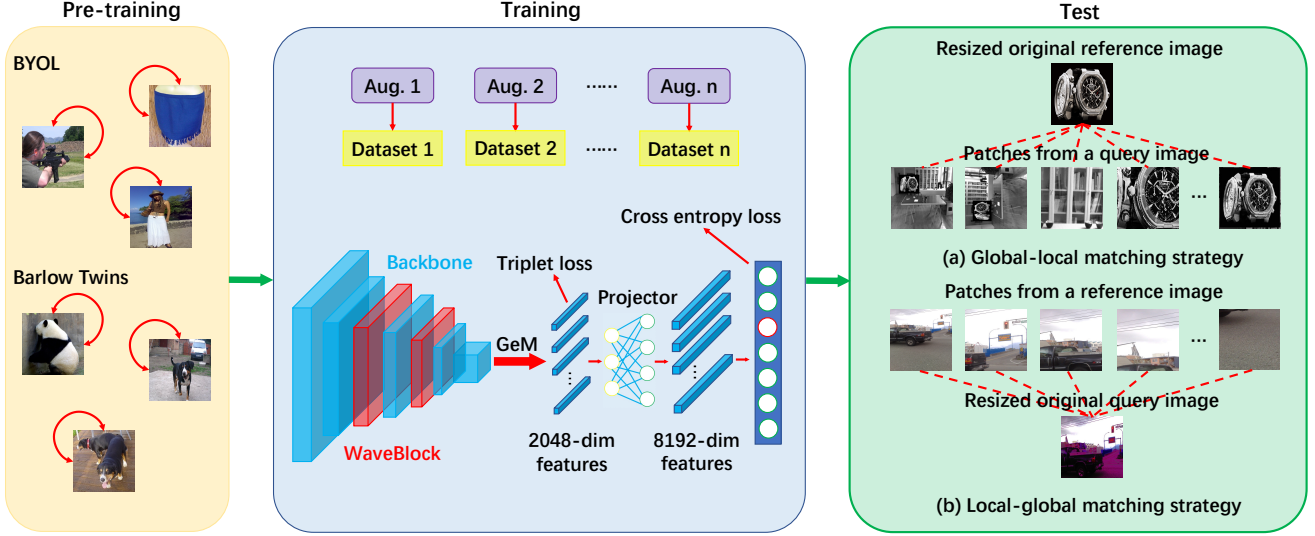


Figure 2. The proposed data-driven and local-verification (D^2LV) approach. Recent self-supervised learning methods, BYOL [13] (its Momentum² Teacher version [19]) and Barlow-Twins [37], are performed for pre-training. During training, we get different trained models by using the combination of basic augmentations with different advanced augmentations separately. When testing, global-local and local-global matching strategy is proposed for the local-verification between reference and query images.

age and b) some queries are cropped from the reference and thus contain only a partial patch of the reference images. In response, both heuristic and auto-detected bounding boxes are adopted to crop some local patches for global-local and local-global matching. The illustration of the proposed approach is shown in Fig. 1.

In summary, the main contributions of this paper are:

1. The paper proposes a data-driven and local-verification approach for image copy detection.
2. The proposed D^2LV approach handles real-life copy detection scenarios in social media well and generalizes well to unseen transformations.
3. Our approach outperforms the baseline models and achieves the state-of-the-art in the Image Similarity Challenge: Matching Track at NeurIPS’21.

2. Related Work

2.1. Copy Detection

Although copy detection plays an important role in social media, the publication of copy detection is not well known because organizations want to keep copy detection techniques obscure, and the researchers often consider that the task is easy [8]. For classical approaches, some methods are used to extract global [16, 32, 12] and local descriptors [1, 3, 15]. For deep learning methods, a descriptor, or known as a feature, is extracted by convolutional neural networks [21, 39]. However, none of them gives a satis-

fying performance on challenging, large benchmarks like ISC2021.

2.2. Unsupervised Pre-training

The unsupervised pre-trained models are from recent self-supervised learning methods. They are trained to extract image embedding unsupervisedly. MoCo [9] builds a dynamic dictionary with a queue and a moving-averaged encoder to conduct contrastive learning. BYOL [13] and its Momentum² Teacher version achieve a new state-of-the-art without negative pairs. Other self-supervised methods, such as Barlow Twins [37], SimSiam [5], and SwAV [4], also show promising performance.

For copy detection in ISC2021, we find that unsupervised pre-trained models show superior performance to their fully-supervised counterparts. That may be because the category defined in unsupervised pre-training is much more similar to that in copy detection than in fully-supervised one.

2.3. Deep Metric Learning

Learning a discriminative feature is a crucial component for many tasks, such as image retrieval [25, 17], face verification [28, 33], and object re-identification [29, 38]. The commonly-used loss functions can be divided into two classes: pair-based [11, 27, 22] and proxy-based [20, 34, 7] losses. Circle loss [28] gives a unified formula for two paradigms.

In our solution to ISC2021, we only use two common losses, *i.e.* triplet loss with hard sample mining and cross-

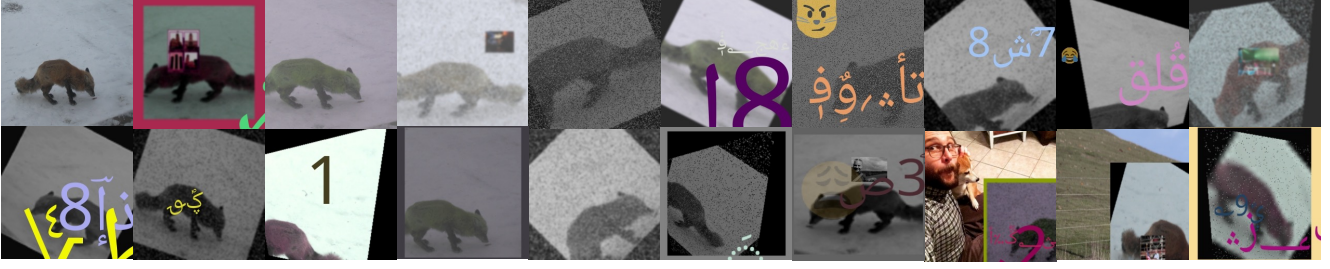


Figure 3. The set of basic augmentations. It includes random resized cropping, random rotation, random pixelization, random pixels shuffling, random perspective transformation, random padding, random image underlay, random color jitter, random blurring, random gray scale, random horizontal flipping, random Emoji overlay, random text overlay, random image overlay, and resizing. The first image is the resized original image.

entropy loss with label smoothing [30]. The two losses are proved to be simple but effective.

3. Proposed Method

In this section, we introduce each important component in the proposed D²LV approach. In the training part, we discuss the built simple but effective baseline and designed different sets of augmentations. In the test part, we discuss the local verification and ensemble methods. The whole approach is shown in Fig. 2.

3.1. Unsupervised Pre-training

In the ISC2021, a category is defined at a very “tight” level, *i.e.* images generated by exact duplication, near-exact duplication, and edited copy are considered in the same category while two images that belong to the same instance or object are not in the same category. However, when using fully-supervised pre-training on the ImageNet, two images share the same instance or object are in one class. Therefore, the definition of the category is contradicted between the ISC2021 and ImageNet.

Fortunately, the recent research on self-supervised learning provides a new direction. It defines every image as a category and uses invariance to data augmentation as their main training criterion [8]. Although it seems natural to directly adopt a self-supervised learning method to train a model for copy detection, we choose to give up this solution for two reasons. First, the self-supervised learning methods often cost a lot of days to get convergence results. For instance, on ImageNet, BYOL [13] or its Momentum² Teacher version [19] takes about two weeks to pre-train 300 epochs with ResNet-152 [10] backbone using 8 NVIDIA Tesla V100 32GB GPUs. In addition, when using sophisticated transformations online, the time becomes much longer, which is unaffordable. Second, even if the resource is unlimited, we do not get a satisfying performance only trained by self-supervised learning methods, which may be

because that the hyper-parameters are not adjusted carefully.

As a result, we choose to use BYOL [13] (its Momentum² Teacher version [19]) and Barlow-Twins [37] to get the pre-trained model on ImageNet. The used augmentations follow the default setting in their original implementations.

3.2. Baseline

We design a simple but effective baseline for ISC2021. Its original version is from DomainMix [35]. The built baseline newly includes GeM [26], WaveBlock [36], a high-dimension projector, two commonly-used losses, and a warming up with cosine annealing learning rate. The backbones selected are ResNet-50 [10], ResNet-152 [10], and ResNet50-IBN [24]. For the design of GeM [26] and WaveBlock [36], please refer to their original papers, and we follow their default hyper-parameters. The high-dimension projector projects a learned 2048-dim feature into 8192-dim via some linear and non-linear connections. We empirically find learning from high dimension space is beneficial for datasets with large-scale categories. The two commonly-used losses are triplet loss with hard sample mining and cross-entropy loss with label smoothing [30]. The 2048-dim feature is used for triplet loss, and the 8192-dim feature is used for classification. The baseline is trained for 25 epochs, and the change of ratio for learning rate is:

$$ratio = \begin{cases} 0.99 \cdot epoch/5 + 0.01, & 0 \leq epoch < 5 \\ 1, & 5 \leq epoch < 10 \\ 0.5 \cdot \left(\cos \left(\frac{epoch-10}{25-10} \cdot \pi \right) + 1 \right), & 10 \leq epoch < 25 \end{cases} \quad (1)$$

3.3. Augmentation

In the ISC2021, the data is crucial in our solution. That is why the proposed approach is named “data-driven”. First, we design a set of basic augmentations to transform images.

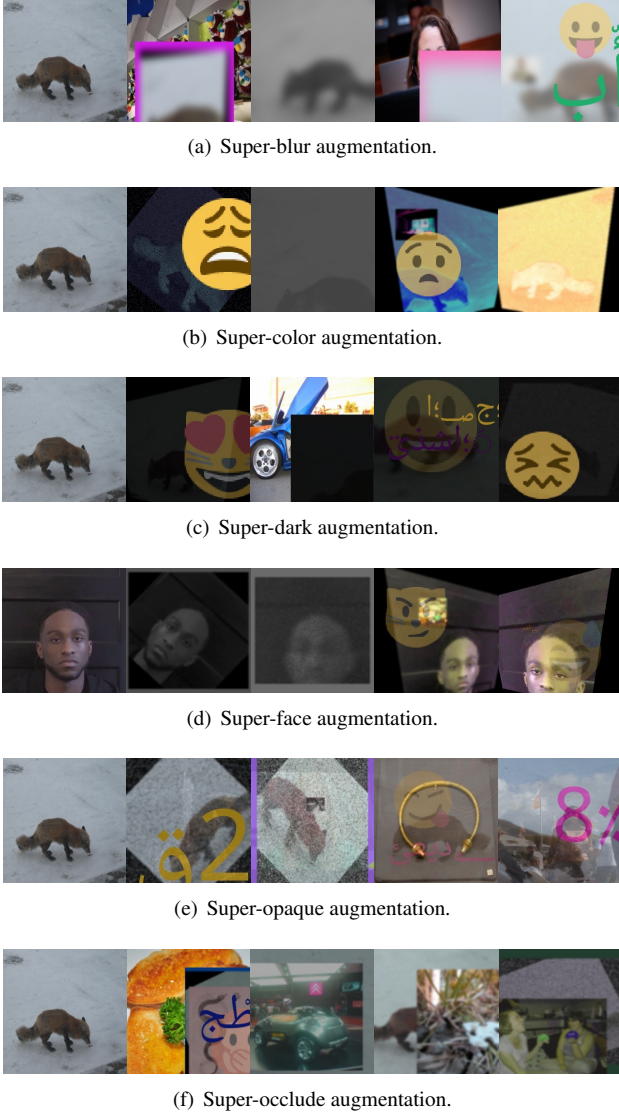


Figure 4. The six advanced augmentations. They are added into the original set of basic augmentations separately. The first image is the resized original image.

Then, we build six advanced augmentations to provide a supplementary.

The set of basic augmentations includes random resized cropping, random rotation, random pixelization, random pixels shuffling, random perspective transformation, random padding, random image underlay, random color jitter, random blurring, random grayscale, random horizontal flipping, random Emoji overlay, random text overlay, random image overlay, and resizing. A display of using all the basic augmentations on one image is shown in Fig. 3. The first image is the resized original image.

Further, together with the set of basic transformations, we design six advanced augmentations, *i.e.* super-

blur, super-color, super-dark, super-face, super-opaque, and super-occlude. The six augmentations are added into the set of basic augmentations *separately*. The super-blur augmentation uses enhanced blur augmentation; the super-color augmentation uses enhanced color jitter augmentation; the super-dark augmentation darkens the images; the super-face augmentation adds some face images into training; the super-opaque augmentation overlays one image on another with certain transparency; the super-occlude augmentation adds more occlusion into original images. These six advanced augmentations are shown in Fig. 4.

Besides the basic and advanced augmentations, we also employ black-white augmentation. The augmentation changes all the color images into black and white style. Some of the sets, *i.e.* “basic”, “basic + super-blur”, “basic + super-color”, and “basic + super-face”, use this augmentation. As a result, we have 11 sets containing different augmentations. A pre-trained model is trained 11 times to get 11 trained models.

3.4. Local Verification

During testing, we observe two corner cases: a) some query images are generated by overlaying a reference image on top of a distractor image. b) some queries are cropped from the reference images and thus only contain parts of the reference images. Therefore, we propose a global-local and local-global matching strategy for testing. For global-local matching, it matches the global features of reference images with local features of query images. For local-global matching, it matches the local features of reference images with global features of query images.

Generating local features of query images. We use heuristic and auto-detected bounding boxes to crop local patches from query images. The features of cropped local patches are used as local features of query images. Given a query image, first, rotating and center cropping are used to generate patches. The rotating degrees are 90° , 180° , and 270° . The center cropping crops not only the “exact center” but also the “1/3 center” of an image. The illustration of “exact center” and “1/3 center” is shown in Fig. 5. Together with the original image, now nine patches are generated. Second, selective search [31] is used to generate proposal regions. The features of proposal regions are also regarded as local features of query images. Last, we use YOLOv5 [14] to detect overlay automatically. For training, we just generate some images with overlay augmentations and corresponding bounding boxes automatically from the training dataset. Note that the above-defined “patch” includes the original image and its rotations.

Generating local features of reference images. We only divide reference images into small patches to match locally. First, given a reference image, it is divided into four parts evenly and nine parts evenly. Then, we crop the “ex-

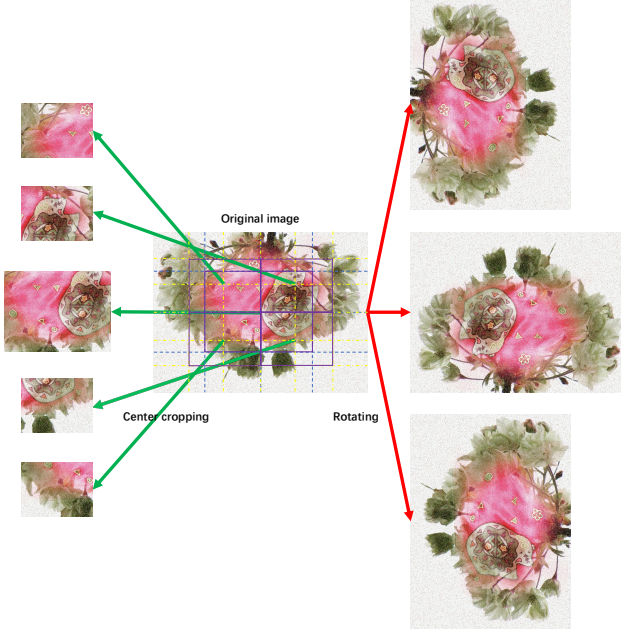


Figure 5. The nine patches generated by rotating and center cropping. The dotted lines in the original image show the definition of “exact center” and “1/3 center”.

act center” and “1/3 center” of a reference image. Together with the original image, we can extract 19 features from a reference image. Note that the above-defined “patch” also includes the original image.

3.5. Ensemble

First, we introduce two ensemble criteria, *i.e.* confidence and completeness. Assume that we have a pair of images, *e.g.* a patch A from a query image and an original reference image B , and two models, f and g . $f(A, B)$ and $g(A, B)$ stand for the similarity score between A and B using models f and g , respectively. Also, two score thresholds are α and β . When using confidence criterion, the ensemble result is:

$$score = \begin{cases} \max(f(A, B), g(A, B)), & \text{if } f(A, B) > \alpha \text{ and } g(A, B) > \beta, \\ None, & \text{others.} \end{cases} \quad (2)$$

The “None” means both the scores are discarded, *i.e.* it does not contribute to the final score of the image pair. Under completeness criterion, the ensemble result is:

$$score = \max(f(A, B), g(A, B)). \quad (3)$$

Both the confidence and completeness criteria can be extended to multi-models by

$$score = \begin{cases} \max(f_0(A, B), f_1(A, B), \dots, f_n(A, B)), & \text{if } f_i(A, B) > \alpha_i, \\ None, & \text{others,} \end{cases} \quad (4)$$

and

$$score = \max(f_0(A, B), f_1(A, B), \dots, f_n(A, B)), \quad (5)$$

where: i is from 0 to n , f_0, f_1, \dots, f_n denotes n different models, and $\alpha_0, \alpha_1, \dots, \alpha_n$ denotes n different score thresholds.

Remember that we have three different backbones, when using the global-local matching strategy, the confidence criterion is used for ResNet50&ResNet152, ResNet50&ResNet50-IBN, and ResNet152&ResNet50-IBN. When using the local-global matching strategy, the confidence criterion is used for ResNet50&ResNet152&ResNet50-IBN. For any other model ensembles, we use the completeness criterion.

Further, to ensemble different local-global and global-local scores, we repeat the completeness criterion by

$$score = \max \left(\begin{matrix} \max(f(A_0, B), f(A_1, B), \dots, f(A_l, B)), \\ \max(f(A, B_0), f(A, B_1), \dots, f(A, B_m)) \end{matrix} \right) \quad (6)$$

where: A_0, A_1, \dots, A_l denotes l different patches of the query image, and B_0, B_1, \dots, B_m denotes m different patches of the reference image.

After finishing all models and patches ensemble, the final score represents the similarity between the pair of images.

4. Experiments

4.1. Experimental Settings

In the unsupervised pre-training part, we essentially follow the experimental setting given in Momentum² Teacher [19] and Barlow-Twins [37]. For Momentum² Teacher [19], the selected backbone is ResNet152 [10] and ResNet50-IBN [24]. 8 NVIDIA Tesla V100 32GB GPUs are used. When training ResNet152 [10], the batch size is 512, and it is trained for 300 epochs. The training process can be finished in about two weeks. When training ResNet50-IBN [24], the batch size is 1024, and it is also trained for 300 epochs. The training process can be finished in about six days. For Barlow-Twins [37], the selected backbone is ResNet50 [10]. We do not re-train the model, and just use the model supplied by the official implement.

In training, we select 100,000 out of 1000,000 images from the official training set. The criterion is selecting one every 10. Each image is augmented 19 times, and thus for training, each ID has 20 images. We trained 33 models in total. Each training takes about/less than one day on 4 NVIDIA Tesla V100 32GB GPUs (bigger backbone takes

Table 1. Comparison with state-of-the-art methods from the leaderboard in the Phase 2. Recall@Precision 90 is a secondary metric provided for information purposes only as an indicator of a model’s recall at a reasonably good precision level, but is not used for ranking purposes. Our results are highlighted in bold.

Team	Score	
	Micro-average Precision	Recall@Precision 90
Ours	0.8329	0.7309
separate	0.8291	0.7917
imgFp	0.7682	0.6715
forthedream	0.7667	0.7218
titanshield	0.7613	0.7557
VisionGroup	0.7169	0.5963
mmcf	0.7107	0.5986
...
MultiGrain[2]	0.2761	0.2023
GIST [23]	0.0526	—

longer and smaller backbone takes shorter). Each training batch includes 128 images of 32 IDs. Adam optimizer [18] is used to optimize the networks. The image size is 256×256 . The model is trained for 25 epochs, and in each epoch, we have 8000 iterations. The basic learning rate is set to 3.5×10^{-4} .

During testing, for global-local matching, we test the 33 trained models for three scales, *i.e.* 200×200 , 256×256 , 320×320 , then ensemble them to get the final results. The time for extracting all query patches’ features using 33 NVIDIA Tesla V100 32GB GPUs is about six hours. For local-global matching, we only test the three models trained on the basic augmentations for one scale, *i.e.* 256×256 . The time for extracting all 19,000,000 reference patches’ features using 3 NVIDIA Tesla A100 40GB GPUs on a DGX-server is less than one day. We apply a PCA dimensionality reduction to decrease dimension from 8192 to 1500 with the code from the competition official. The 1500-dim feature is used for final matching. Besides, some tricks are used to further improve performance. First, when performing local-global strategy, it is inappropriate to divide reference images containing faces into patches. Therefore, when a face detector finds face(s) existing in one reference image, we do not perform the local-global strategy. Second, compared to original images, the partial image in a pair is more likely to be “false positive”, and thus we penalize the corresponding score. Third, we delete generated query patches with too small image size. Fourth, the final ensemble score uses the average of two maximum scores instead of the only one as introduced before.

4.2. Comparison with State-of-the-Arts

To prove the superiority of the D²LV, we compare the proposed model with state-of-the-art methods from the leaderboard in Phase 2. The comparison results are shown

Table 2. The ablation study about the proposed D²LV. “Supervised” or “Unsupervised” denotes the supervised pre-training or unsupervised pre-training is used, respectively. “Global-local” denotes using global-local matching strategy, and “Both” denotes using global-local and local-global matching strategy. “Adv-Aug” denotes using different kinds of advanced augmentations. “Multi+Tricks” denotes using multi-scale testing and other mentioned tricks. The best results are highlighted in bold.

Method	Score	
	Micro-average Precision	Recall@Precision 90
Supervised	0.68726	0.54678
Unsupervised	0.70813	0.62773
Global-local	0.82726	0.74755
Both	0.83720	0.75155
Adv-Aug	0.88640	0.80124
Multi+Tricks	0.90035	0.81887

in Table 1. In the ISC2021, there are 1103 participants, and 36 teams have submitted their final results. Compared with the strongest official benchmark MultiGrain [2], the proposed D²LV achieves about 56% improvements, which is considerable. Most Micro-average Precisions from other teams are less than 77%, while our approach gives an 83.29% result. It is interesting to mention that, in Phase 1, our result is 90.08%. There is only a less than 7% gap between the two leaderboards for us. However, for some other teams, the gap can be larger than 30%. The superiority performance is attributed to two aspects. First, the sophisticated augmentations give us more generalizability when facing unseen transformations. That is called “Data-Driven”. Second, the global-local and local-global matching strategy provides an exhaustive matching between a pair of images. That is called “Local-Verification”.

4.3. Ablation Studies

The ablation studies are conducted on 25,000 query images in Phase 1 to prove the effectiveness of each component in the D²LV approach. The evaluation metric is Micro-average Precision. The experimental results are displayed in Table 2.

Comparison between supervised pre-training and unsupervised pre-training. First, we discuss the improvement brought by unsupervised pre-training. The experimental results are denoted as “Supervised” and “Unsupervised” in Table 2, respectively. The training images only use the basic augmentations. The matching strategy is only global-to-global. We can find that, instead of supervised pre-training, 2.1% improvement has been obtained by using unsupervised pre-trained models. This phenomenon may be because the definition of category in unsupervised pre-training is similar to that in the task of copy detection.

The improvement from local-verification. In this part, the experimental results are from the ensemble result of the

three backbones. The experimental results are denoted as “Global-local” and “Both” in Table 2, respectively. When only using the global-local matching strategy, the performance can be improved from 70.81% to 82.73%. When we perform global-local and local-global matching strategy, the highest performance, *i.e.* 83.72%, is achieved. The local-verification plays a very important role in the proposed D²LV.

The improvement from advanced augmentations. To be convenient, we only give the final ensemble experimental results of all the advanced augmentations with the basic ones. The experimental results are denoted as “Adv-Aug” in Table 2. Indeed, each advanced augmentation with the basic one can improve performance separately. Also, the results use local-verification and three backbones. The sophisticated augmentations contribute a lot to Phase 2 where some unseen transformations appear.

The improvement from multi-scale testing and some tricks. The experimental results are denoted as “Multi+Tricks” in Table 2. The performance improved by multi-scale testing and some tricks is not very significant. It is less than 1.5% on 25,000 queries in Phase 1. After finding the huge performance gap between the two phases, we are not quite sure whether these methods really contribute to the final results in Phase 2.

5. Conclusion

In this paper, we introduce our winning solution to Image Similarity Challenge: Matching Track at NeurIPS’21. The proposed D²LV approach uses recent self-supervised learning methods for pre-training instead of traditional supervised ones. Further, we find that exploring data is of great importance, and thus many strong augmentations are designed. Also, the proposed global-local and local-global matching strategy contributes a lot to the final submission. We hope the proposed solution is beneficial for real-life applications including content tracing, copyright infringement, and misinformation.

References

- [1] Laurent Amsaleg and Patrick Gros. Content-based retrieval using local descriptors: Problems and issues from a database perspective. *Pattern Analysis & Applications*, 4(2):108–124, 2001. 2
- [2] Maxim Berman, Hervé Jégou, Vedaldi Andrea, Iasonas Kokkinos, and Matthijs Douze. MultiGrain: a unified image embedding for classes and instances. *arXiv e-prints*, Feb 2019. 6
- [3] Sid-Ahmed Berrani, Laurent Amsaleg, and Patrick Gros. Robust content-based image searches for copyright protection. In *Proceedings of the 1st ACM international workshop on Multimedia databases*, pages 70–77, 2003. 2
- [4] Mathilde Caron, Ishan Misra, Julien Mairal, Priya Goyal, Piotr Bojanowski, and Armand Joulin. Unsupervised learning of visual features by contrasting cluster assignments. 2020. 2
- [5] Xinlei Chen and Kaiming He. Exploring simple siamese representation learning. In *Proceedings of the IEEE/CVF Conference on Computer Vision and Pattern Recognition*, pages 15750–15758, 2021. 2
- [6] Jia Deng, Wei Dong, Richard Socher, Li-Jia Li, Kai Li, and Li Fei-Fei. Imagenet: A large-scale hierarchical image database. In *2009 IEEE conference on computer vision and pattern recognition*, pages 248–255. Ieee, 2009. 1
- [7] Jiankang Deng, Jia Guo, Niannan Xue, and Stefanos Zafeiriou. Arcface: Additive angular margin loss for deep face recognition. In *Proceedings of the IEEE/CVF Conference on Computer Vision and Pattern Recognition*, pages 4690–4699, 2019. 2
- [8] Matthijs Douze, Giorgos Tolias, Ed Pizzi, Zoë Papakipos, Lowik Chanussot, Filip Radenovic, Tomas Jenicek, Maxim Maximov, Laura Leal-Taixé, Ismail Elezi, et al. The 2021 image similarity dataset and challenge. *arXiv preprint arXiv:2106.09672*, 2021. 1, 2, 3
- [9] Kaiming He, Haoqi Fan, Yuxin Wu, Saining Xie, and Ross Girshick. Momentum contrast for unsupervised visual representation learning. In *Proceedings of the IEEE/CVF Conference on Computer Vision and Pattern Recognition*, pages 9729–9738, 2020. 2
- [10] Kaiming He, Xiangyu Zhang, Shaoqing Ren, and Jian Sun. Deep residual learning for image recognition. In *Proceedings of the IEEE conference on computer vision and pattern recognition*, pages 770–778, 2016. 3, 5
- [11] Alexander Hermans, Lucas Beyer, and Bastian Leibe. In defense of the triplet loss for person re-identification. *arXiv preprint arXiv:1703.07737*, 2017. 2
- [12] Jen-Hao Hsiao, Chu-Song Chen, Lee-Feng Chien, and Ming-Syan Chen. A new approach to image copy detection based on extended feature sets. *IEEE Transactions on Image Processing*, 16(8):2069–2079, 2007. 2
- [13] Grill Jean-Bastien, Strub Florian, Alché Florent, Tallec Corentin, Pierre Richemond H., Buchatskaya Elena, Doersch Carl, Bernardo Pires Avila, Zhaohan Guo Daniel, Mohammad Azar Gheshlaghi, Piot Bilal, Kavukcuoglu Koray, Munos Rémi, and Valko Michal. Bootstrap your own latent - a new approach to self-supervised learning. *NIPS 2020*, 2020. 1, 2, 3
- [14] Glenn Jocher. ultralytics/yolov5: v3.1 - Bug Fixes and Performance Improvements. <https://github.com/ultralytics/yolov5>, Oct. 2020. 4
- [15] Yan Ke, Rahul Sukthankar, and Larry Huston. Efficient near-duplicate detection and sub-image retrieval. In *ACM multimedia*, volume 4, page 5. Citeseer, 2004. 2
- [16] Changick Kim. Content-based image copy detection. *Signal Processing: Image Communication*, 18(3):169–184, 2003. 2
- [17] Sungyeon Kim, Dongwon Kim, Minsu Cho, and Suha Kwak. Proxy anchor loss for deep metric learning. In *Proceedings of the IEEE/CVF Conference on Computer Vision and Pattern Recognition*, pages 3238–3247, 2020. 2

- [18] Diederik P. Kingma and Jimmy Ba. Adam: A method for stochastic optimization. In *ICLR (Poster)*, 2015. 6
- [19] Zeming Li, Songtao Liu, and Jian Sun. Momentum⁺ 2 teacher: Momentum teacher with momentum statistics for self-supervised learning. *arXiv preprint arXiv:2101.07525*, 2021. 1, 2, 3, 5
- [20] Weiyang Liu, Yandong Wen, Zhiding Yu, Ming Li, Bhiksha Raj, and Le Song. Sphreface: Deep hypersphere embedding for face recognition. In *The IEEE Conference on Computer Vision and Pattern Recognition (CVPR)*, 2017. 2
- [21] Xiaolong Liu, Jinchao Liang, Zi-Yi Wang, Yi-Te Tsai, Chia-Chen Lin, and Chih-Cheng Chen. Content-based image copy detection using convolutional neural network. *Electronics*, 9(12):2029, 2020. 2
- [22] Hyun Oh Song, Yu Xiang, Stefanie Jegelka, and Silvio Savarese. Deep metric learning via lifted structured feature embedding. In *Proceedings of the IEEE conference on computer vision and pattern recognition*, pages 4004–4012, 2016. 2
- [23] Aude Oliva and Antonio Torralba. Modeling the shape of the scene: A holistic representation of the spatial envelope. *International journal of computer vision*, 42(3):145–175, 2001. 6
- [24] Xingang Pan, Ping Luo, Jianping Shi, and Xiaoou Tang. Two at once: Enhancing learning and generalization capacities via ibn-net. In *Proceedings of the European Conference on Computer Vision (ECCV)*, September 2018. 3, 5
- [25] Qi Qian, Lei Shang, Baigui Sun, Juhua Hu, Hao Li, and Rong Jin. Softtriple loss: Deep metric learning without triplet sampling. In *Proceedings of the IEEE/CVF International Conference on Computer Vision*, pages 6450–6458, 2019. 2
- [26] Filip Radenović, Giorgos Tolias, and Ondřej Chum. Fine-tuning cnn image retrieval with no human annotation. *IEEE transactions on pattern analysis and machine intelligence*, 41(7):1655–1668, 2018. 3
- [27] Kihyuk Sohn. Improved deep metric learning with multi-class n-pair loss objective. In *Advances in neural information processing systems*, pages 1857–1865, 2016. 2
- [28] Yifan Sun, Changmao Cheng, Yuhao Zhang, Chi Zhang, Liang Zheng, Zhongdao Wang, and Yichen Wei. Circle loss: A unified perspective of pair similarity optimization. In *Proceedings of the IEEE/CVF Conference on Computer Vision and Pattern Recognition (CVPR)*, June 2020. 2
- [29] Yifan Sun, Liang Zheng, Yi Yang, Qi Tian, and Shengjin Wang. Beyond part models: Person retrieval with refined part pooling (and a strong convolutional baseline). In *Proceedings of the European conference on computer vision (ECCV)*, pages 480–496, 2018. 2
- [30] Christian Szegedy, Vincent Vanhoucke, Sergey Ioffe, Jon Shlens, and Zbigniew Wojna. Rethinking the inception architecture for computer vision. In *Proceedings of the IEEE conference on computer vision and pattern recognition*, pages 2818–2826, 2016. 3
- [31] Jasper RR Uijlings, Koen EA Van De Sande, Theo Gevers, and Arnold WM Smeulders. Selective search for object recognition. *International journal of computer vision*, 104(2):154–171, 2013. 4
- [32] YH Wan, QL Yuan, SM Ji, LM He, and YL Wang. A survey of the image copy detection. In *2008 IEEE Conference on Cybernetics and Intelligent Systems*, pages 738–743. IEEE, 2008. 2
- [33] Feng Wang, Xiang Xiang, Jian Cheng, and Alan Loddon Yuille. Normface: L2 hypersphere embedding for face verification. In *Proceedings of the 25th ACM international conference on Multimedia*, pages 1041–1049, 2017. 2
- [34] Hao Wang, Yitong Wang, Zheng Zhou, Xing Ji, Dihong Gong, Jingchao Zhou, Zhifeng Li, and Wei Liu. Cosface: Large margin cosine loss for deep face recognition. In *Proceedings of the IEEE conference on computer vision and pattern recognition*, pages 5265–5274, 2018. 2
- [35] Wenhao Wang, Shengcai Liao, Fang Zhao, Kangkang Cui, and Ling Shao. Domainmix: Learning generalizable person re-identification without human annotations. In *British Machine Vision Conference*, 2021. 3
- [36] Wenhao Wang, Fang Zhao, Shengcai Liao, and Ling Shao. Attentive waveblock: Complementarity-enhanced mutual networks for unsupervised domain adaptation in person re-identification and beyond. *arXiv preprint arXiv:2006.06525*, 2020. 3
- [37] Jure Zbontar, Li Jing, Ishan Misra, Yann LeCun, and Stéphane Deny. Barlow twins: Self-supervised learning via redundancy reduction. In *ICML*, 2021. 1, 2, 3, 5
- [38] Zhedong Zheng, Tao Ruan, Yunchao Wei, Yi Yang, and Tao Mei. Vehiclenet: Learning robust visual representation for vehicle re-identification. *IEEE Transactions on Multimedia*, 2020. 2
- [39] Zhili Zhou, Meimin Wang, Yi Cao, and Yuecheng Su. Cnn feature-based image copy detection with contextual hash embedding. *Mathematics*, 8(7):1172, 2020. 2